

# Improved region growing method for magnetic resonance images (MRIs) segmentation

E. A. Zanaty

Department of Computer Science, Faculty of Science, Sohag University, Sohag City, Egypt

**Email address:**

zanaty22@yahoo.com

**To cite this article:**

E. A. Zanaty. Improved Region Growing Method for Magnetic Resonance Images (MRIs) Segmentation, *American Journal of Remote Sensing*. Vol. 1, No. 2, 2013, pp. 53-60. doi: 10.11648/j.ajrs.20130102.16

---

**Abstract:** Segmentation of magnetic resonance images (MRIs) is challenging due to the poor image contrast and artifacts that result in missing tissue boundaries, i.e. pixels inside the region and on the boundaries have similar intensity. In this paper, we adapt a region growing method to segment MRIs which contain weak boundaries between different tissues. The proposed region growing algorithm is developed to learn its homogeneity criterion automatically from characteristics of the region to be segmented. An automatic homogeneity criterion based on estimating probability of pixel intensities of a given image is described. The homogeneity criteria as well as the probability are calculated for each pixel. The proposed algorithm selects the pixels sequentially in a random walk starting at the seed point, and the homogeneity criterion is updated continuously. The proposed algorithm is applied to challenging applications: gray matter/white matter segmentation in magnetic resonance image (MRI) datasets. The experimental results show that the proposed technique produces accurate and stable results.

**Keywords:** Mris, Image Segmentation, Region Growing, Probability

---

## 1. Introduction

Medical imaging includes conventional projection radiography, computed tomography (CT), magnetic resonance imaging (MRI), and ultrasound. MRI has several advantages over other imaging techniques enabling it to provide 3D data with high contrasts between soft tissues [1]. However, the amount of data is far too much for manual analysis/interpretation, and this has been one of the biggest obstacles in the effective use of MRI. The segmentation of medical images is an important first step for variety image related application and visualization tasks. It provides assistance for medical doctors to find out the diseases inside the body without the surgery procedure, to reduce the image reading time, to find the location of a lesion, and to determine an estimate of the probability of a disease. There are many types of image segmentation techniques [2-3]. Among them, histogram-based [4-6] and region-based [7-11] techniques are most popular.

The histogram techniques [4-6] had been tried to solve threshold problem in histogram- and region-based methods. However, it is really difficult to find a general threshold for all cases to determine the threshold value for segmentation. In [5], the histogram-based segmentation technique pro-

duces a binary image based on the threshold value. The intensities of object and background pixels tend to cluster into two sets in the histogram with threshold between these two sets. An approach was proposed by Tobias and Seara [6] to threshold the histogram according to the similarity between gray levels. Such a similarity is assessed through a fuzzy measure. This approach was presented to overcome the local minima that affect most of the conventional methods. Chen [4] presented a technique based on partitioning the histogram and interval thresholding for volumetric breast tissue segmentation. Based on its distribution shape, the histogram is partitioned by either a valley-seeking algorithm (for multimodal) or a five-subinterval algorithm (for unimodal). Applied to volumetric breast analysis, this technique decomposes a breast volume into five sub-volumes corresponding to five intensity subintervals: lower (air bubble), low (fat), middle (normal tissue, or parenchyma), high (glandular duct), higher (calcification), in the order of X-ray attenuation value.

The region-based segmentation techniques segment an image which has strong boundaries into several small regions, followed by merge procedure using specific threshold. These techniques have focused on the design of the growing criteria as well as on algorithm efficiency [3].

Methods can be categorized into:

- Criterion selection based on gray-level properties of the current points [7-9]. These methods are dependent on seed point location and search order. They concern by selecting a pixel for image segmentation and its improvements. The first method is called "Seeded Region Growing" and it is introduced by Adams and Bischof [7] and the improved version of this algorithm was proposed in [8] which often determine the final segmentation results by subsequent region grow. As described in [9, 10], the seeded region growing (SRG) has two inherent pixel order dependencies that cause different resulting segments. The first-order dependency occurs whenever several pixels have the same difference measure to their neighbouring regions. The second-order dependency occurs when one pixel has the same difference measure to several regions. Wu et al. [11] proposed a new texture feature-based seeded region growing algorithm for automated segmentation of organs in abdominal magnetic resonance images (MRIs). Co-occurrence texture feature and semi-variogram texture feature are extracted from the image and the seeded region growing algorithm is run on these feature spaces. With a given Region of Interest (ROI), a seed point is automatically picked up based on three homogeneity criteria. A threshold is then obtained by taking a lower value just before the one causing 'explosion'.

- Segmentations using different homogeneity criterion [12-16]. Methods are often slow because of the large number of segmentations and they require distinguishing the true result from segmentations with slightly different homogeneity criteria. Ayman et al. [12] presented region growing (RG) technique for medical image segmentation. Their algorithm is based on a homogeneity threshold for improve region growing. Although the algorithm works well in high noises and achieves similar results as Del-Fresno et al. [14] in case of low noise levels, more discussions can be shown in [12], it suffers misclassification tissues of images that include weak boundaries. Wang et al. [13] performed image segmentation on the whole image by doing boundary detection and region merging iteratively. However, Canny edge detection is adopted to evaluate the performance of edges locating and decide which is the most suitable. Wu et al. [15] described a top down region-based image segmentation technique for medical images that contain three major regions: background and two tissues. This method can only segment 2D images and cannot segment 3D images or images which contain more than two tissues.

- Criterion selection for a complete segmentation of the scene with potentially varying criterion for different regions [16-17]. The techniques combine two or more methods for segmenting the complete image which is based on a notion of overall optimality. Tang et al. [16] presented an MRI brain image segmentation approach based on multiresolution edge detection, region selection, and intensity threshold techniques. To obtain more accurate tissue segmentation, region growing was hybridized with genetic as in [17]

and Harris detection as in [18]. Although the quality of image segmentation is improved, they consumed much time for finding the optima. Moreover, the previous algorithms had suppressed the impact of noise and intensity inhomogeneity to some extent, these algorithms still produces misclassified small regions.

Since MRIs with weak boundaries have very similar pixels value around the boundaries, it is difficult to segment the tissues of white matter (WM) and gray matter (GM). Furthermore, region growing method cannot specifically segment the tissues because the growing of the region will not stop on the boundaries and will add outside pixels of the tissue to the organ. The region growing always used human users' intervention by selecting initial seeds manually [11], the problem here is that the selection of homogeneity criterion is very important for influencing the accuracy of final segmentation especially with weak boundaries MRIs segmentation.

In this paper, we present an automatic region growing technique capable to segment tissues with weak boundaries. We designed a new process of region growing for segmenting complex structures that overcomes the limitations of homogeneity criterion. The process estimates the homogeneity criterion from the image itself over the image as a function of intensity probability to provide better segmentation results. The efficiency of proposed algorithm is demonstrated by extensive segmentation experiments using real MRIs, compared with other state of the art algorithms.

The rest of the paper is organized as follows. The MRI segmentation problem is discussed in Section 2. The proposed region growing method is described in Section 3. The experimental results are presented in Section 4. Our conclusion is presented in Section 5.

## 2. Weak Boundary MRI Segmentation

The basic idea of image segmentation can be described as follows. Given a set of data  $X = \{x_1, x_2, \dots, x_N\}$  and uniformity predicates  $P$ , we desire to obtain a partition of the data into disjoint nonempty groups  $X = \{v_1, v_2, \dots, v_k\}$  subject to the following conditions:

- (1)  $\bigcup_{i=1}^k v_i = X$
- (2)  $v_i \cap v_j = \emptyset, i \neq j$
- (3)  $P(v_i) = TRUE, i = 1, 2, \dots, k$
- (4)  $P(v_i \cup v_j) = FALSE, i \neq j$

The first condition ensures that every data value must be assigned to a group, while the second condition ensures that a data value can be assigned to only one group. The third and fourth conditions imply that every data value in one group must satisfy the uniformity predicate while data values from two different groups must fail the uniformity criterion.

MRIs segmentation involves the separation of image pixels into regions comprising different tissue type. All MRIs are affected by random noise. The noise comes from

the stray current in the detector coil due to the fluctuating magnetic fields arising from random ionic currents in the body, or the thermal fluctuations in the detector coil itself [1]. When the level of noise is significant in an MR image, tissues that are similar in contrast could not be delineated effectively, causing error in tissue segmentation. In MRIs, intensity non-uniformity can affect computational analysis of the image due to the variance in signal intensity. It is manifested as smooth spatially varying signal intensity across the image and caused by several factors including inhomogeneous radiofrequency (RF) fields (caused by distortion of the RF field by the object being scanned or non-uniformity of the transmission field). The boundaries among tissues become weak when RF and noise increase. Furthermore, inside each tissue the pixels of the region have very similar intensities and outside each tissue the pixels have different intensities from inside the region. Also, the pixels on the boundaries will have intensities between the intensities inside and outside. The boundaries become strong if there is big difference between the pixels inside and outside the tissues, and become weak if the difference is small.

In both cases, the pixels intensities on the boundaries have different values from inside and outside pixels intensities. Furthermore, the numbers of pixels which have the same intensity inside or outside the tissue(s) are much bigger than the number of pixels on the boundaries. So, probabilities of these pixels intensities in the tissue or in the other tissues have higher value than pixels intensities on the boundaries.

### 3. Adapting Region Growing Method (RG)

The region growing (RG) is an approach to image segmentation in which neighboring pixels are examined and added to a region class [12-16]. This technique used only a few seed pixels as “object”, and described each pixel in the object to belong to the object or belong to the edges of this object. The major problems of RG are related to selecting a threshold capable to segment images containing weak boundaries.

The simple RG technique consists in merging neighboring pixels  $P_x$  to pixels  $P_y$  inside the region, according to  $|I(P_x) - I(P_y)| \leq T$ , where T is a fixed threshold and  $I(\bullet)$  is the pixel intensity value. This technique has two problems, 1) the choice of the threshold and 2) this technique can lead to a chaining effect especially for image with pixel intensity changing gradually. The second problem can be solved by using the homogeneity test  $f(I_{i,j}) = |I_{i,j} - RA| \leq T$ , where RA is the average pixel (the summation of pixels intensities over the number of pixels inside the region). These problems are addressed and solved in the next subsections to achieve high segmentation accuracy of weak boundaries images. This technique uses dif-

ferent fixed thresholds for each tissue in the image. The fixed threshold crosses the function  $f(I_{i,j})$  between two points ( $a < RA$  and  $b > RA$ ) with the same distant from RA, if T is a small a prescribed value, then pixels inside the tissue will be described as outside, and if it is big, some pixels outside the tissue will be added to the region especially when the tissue has weak boundaries.

In this section, the RG technique is proposed for extracting only the tissue which the user will choose. The threshold of RG is selected as a function of probability of image pixels to determine a suitable regions cut especially when weak boundaries are found. The threshold will be calculated for each pixel inside the region by using probability of pixel intensity  $Pr(I_{i,j})$ , pixel intensity value  $I_{i,j}$ , and pixel neighbors  $Ne(I_{i,j})$ . We suppose that:

$$|I_{i,j} - RA| \leq T(I_{i,j}, Pr(I_{i,j}), Ne(I_{i,j})) \tag{1}$$

Since the pixels that are of very similar values need a small threshold T, the distances  $|I_{i,j} - RA|$  are very small for the pixels near to boundaries. To extract a tissue around the weak boundaries, the region should be stopping growing when it meets these boundaries. For that, we define the threshold function as follows:

$$T = T_1(I_{i,j}, Pr(I_{i,j})) + T_2(Pr(I_{i,j}), Ne(I_{i,j})), 0 < I_{i,j} < 1 \tag{2}$$

Eq.(2) consists of two terms. The first term is fixed for all pixels in the image that have the same intensity and therefore it has the same  $Pr(I_{i,j})$ , so we can define it as global threshold  $T_1$ . The second term of T depends on  $Pr(I_{i,j})$  and the pixels neighborhood  $Ne(I_{i,j})$ , so we can define it as local threshold  $T_2$ . We assume that  $T_1$  is a combination of  $Pr(I_{i,j})$  and  $I_{i,j}$ . This function will increase when  $Pr(I_{i,j})$  decreases. Therefore, we can define  $T_1$  as:

$$T_1(I_{i,j}, Pr(I_{i,j})) = I_{i,j}^{2\alpha} e^{-2\beta} \tag{3}$$

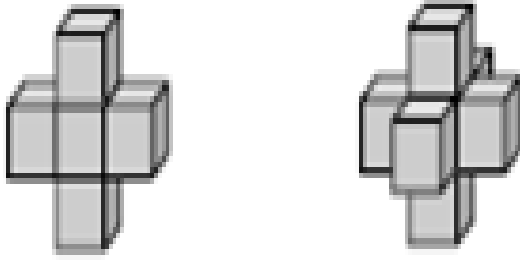
where  $\beta = [\log(Pr(I_{i,j}))]^{-1}$  and  $\alpha = (2.6 + \alpha_1) I_{i,j}^{1/2}$ .  $T_1$  will give us homogenous threshold and will decrease when increases. We choose  $\alpha$  to decrease T1 when  $I_{i,j}$  increases.  $\alpha_1$  is a prescribed value. From our experiments, we found that there are some pixels in the tissue that give high value  $Pr(I_{i,j})$ , therefore the left side of Eq.(1) has higher values than T (if  $T = T_1$ ), so these pixels need additional threshold to be in the region. In this case, we use  $T_2$  to increase T.

The region should be stopping to grow at the weak boundaries. For that  $T_2$  is selected to be smaller value on weak boundaries than inside the tissue. On the other hand,  $T_2$  is yield to zero i.e.  $\sum_{k,l} |I_{i+k,j+l} - Med| \Rightarrow 0$ ,  $Med$  is the

median of these pixels at pixels with same values, it has big values for non-similar pixels of tissues, and it will be increased when pixels have higher  $\Pr(I_{i,j})$ . We define  $T_2$  as:

$$T_2(\Pr(I_{i,j}), Ne(I_{i,j})) = \frac{4\beta}{(n-1)^2} \sum_{k,l} |I_{i+k,j+l} - Med| \quad (4)$$

Where  $n$  is the number of pixels,  $k=0$  when  $l=\pm 1$  and  $l=0$  when  $k=\pm 1$  with  $n=5$  and for  $n=9$ ,  $k=l=0, \pm 1$ .  $T_2$  will be almost zero in very similar parts since the summation will be almost zero and bigger if the pixel  $I_{i,j}$  has different neighbor's intensity value. We can calculate  $T_1$  and  $T_2$  from Eq.(3) and Eq.(4) respectively. The pixels neighbors in 2D and 3D are 4 or 8 pixels respectively as shown in Figure 1. Then the  $T$  threshold can be computed from Eq.(1) to examine the neighboring pixels to the seed. The behavior of  $T_1$  and  $T_2$  corresponding to the histogram can be described in Figure 2.  $T_1$  and  $T_2$  take small value at peaks of the histogram and growth according histogram.  $T$  yields to zero at top or bottom of the peaks.



2D neighbors      3D neighbors  
**Figure 1:** Pixel and its neighbors for 2D and 3D.

In fact,  $T$  function is fixed for all pixels in the image, which have the same intensity since it has also the same  $\Pr(I_i)$ . We will use  $T_1$  to find forward very dark pixel intensity that is outside the tissue. Furthermore,  $T_2$  takes smallest value when pixels intensities have highest probability from the whole image for a tissue since these pixels must be very similar part. Therefore, this function will increase when  $\Pr(I_i)$  decreases to help  $T_1$  to find  $I_i$  such that  $T < f(I_i)$ . The proposed algorithm starts by determining the set of seeds  $S = \{I_i \mid i = 1, 2, \dots, N\}$ . As in the step 3 of the proposed algorithm (shown below), we select the initial seed  $I_1$  and put this seed into  $R_k$  and then delete it from  $S$ . By selecting  $I_1$ , the algorithm grows until satisfying Eq.(1) through Eqs.(2-4). Select the second seed  $I_2$  and do step 3 again and so on for getting all seeds.

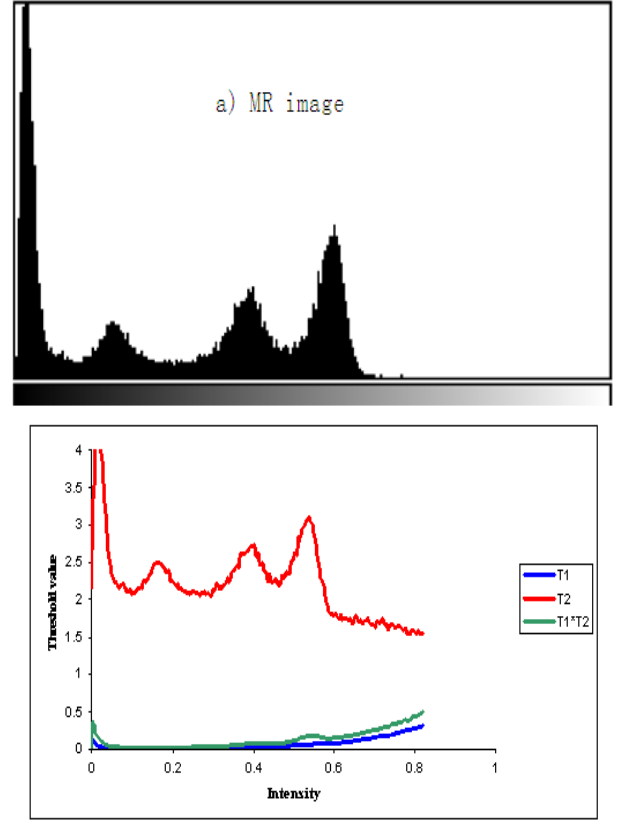


**Figure 2:** The relation between thresholds ( $T_1$  and  $T_2$ ) and intensity for histogram segmentation slice#65 using region growing algorithm based on (PN).

The steps of the proposed algorithm can be described as follows:

Algorithm:

Input: MRI images and seed pixel(s).

Tune: The parameters  $\beta_1$  and  $\gamma_1$ .

Outputs: The set of regions.

Begin:

- 1- Read the images and select seed pixel(s).
- 2- Let  $S = \{I_i \mid i = 1, 2, \dots, N\}$  be the set of seed pixel(s) and set the counter  $k := 0$ .
- 3- Main Loop, while  $S \neq \emptyset$ , do the following steps
  - 3.1-3.9.
    - 3.1 Set  $k := k + 1$ ,  $R_k = \emptyset$ ,  $RA = 0$  and  $J = \emptyset$ .
    - 3.2 Choose a seed  $I_k \in S$ .
    - 3.3 Update  $S$ , where  $S = S - \{I_k\}$ .
    - 3.4 Update  $R_k$ , where  $R_k = R_k \cup \{I_k\}$ .
    - 3.5 Update  $RA$ , where  $RA = \text{average}(\{RA\} \cup \{I_k\})$ .
    - 3.6 Update  $J$ , where  $J = J \cup \text{neighbors}(I_k)$ .
    - 3.7 Compute  $f(J)$ , where  $f(J) = \{|RA - I_i|, I_i \in J\}$ , and set  $Z = \{J_i \mid f(J_i) = \min(f(J))\}$ .
    - 3.8 If  $Z$  satisfy Eq.(1) (Eqs.(2-4)), then set  $I_k = Z$ .
    - 3.9 Update  $J$ , where  $J = J - \{I_k\}$  and go to Step 3.3.
- 4- Stop.
- 5- Return the regions  $R_i$ ,  $i = 1, 2, \dots, k$ .
- 6- End.

## 4. Experimental and Comparative Results

The experiments were performed with several data sets using MATLAB. We apply the proposed technique to T1-weighted MRI phantom with slice thickness of 1mm, generated at various noise levels and spatial intensity non-uniformity (RF) levels [19] and [20]. The advantages of using digital phantoms rather than real image data for validating segmentation methods include prior knowledge of the true tissue types and control over image parameters such as modality, slice thickness, noise and intensity inhomogeneities. We use 4 and 6 neighbors for 2D and 3D respectively. The size of the seeded region is a window of  $3 \times 3$ . In our algorithm, we set the parameters  $\gamma_1 = \alpha_1 = 3.2$  and  $\beta_1 = 2.2$ .

To demonstrate the advantage of the proposed approach over the other techniques in terms of accuracy, we use average overlap metric (AOM) [21] as a metric to evaluate the performance of image segmentation algorithms. The AOM is computed as follows:

$$\text{AOM}(A, B) = 2|A \cap B| / (|A| + |B|),$$

where A represents the set of results obtained by the proposed technique and B represents the set of the ground truth data. These metrics reach a value of 1.0 for results that are very similar and is near 0.0 when they share no similarly classified voxels.

### 4.1. Experiment on MRI

In this section, slice#62 and slice#63 are used with slice thickness of 1mm, 3% noise and no intensity inhomogeneities. They are obtained from the classical simulated brain database of McGill University [19]. The initial seed of the images is selected by capturing the pixel by mouse (press the mouse pointer on the seed pixel). As shown in Figure 3, the proposed method is succeeded to extract the white matter (WM) from slice#62 and slice#63. The segmentation accuracy of both exceeds 91%.

Next test, the proposed technique is applied to slice#62 at various noise levels (0%, 3%, 7% and 9%) and spatial RF levels (0% and 20%) as shown in Figure 4. Figure 4 shows the segmentation accuracy of WM of original slice#62 with different noise and RF levels. To prove the efficiency of proposed algorithm, several noise levels are added to this data set, while AOM average is evaluated. Table 1 shows AOM of WM with the proposed algorithm applied to MRI image with various noise levels (0%, 3%, 5%, 7%, 9%) and RF levels (0% and 20%). The obtained results show that the proposed algorithms are very robust to noise and intensity homogeneities and inhomogeneities. The segmentation accuracy (using AOM) is evaluated. According to Zijdenbos [22] statement that  $\text{AOM} > 0.7$  indicates excellent agreement; the proposed algorithm has desired performance in cortical segmentation. The best AOM is achieved for low noise and RF levels, for which values of

AOM are higher than 0.97. According to Table 1, the proposed technique is stable at 90% at noise level 9% and RF 40%, this result is satisfactory for segmenting the WM tissues.

### 4.2. Comparative Results

In this section, the proposed method is evaluated and compared to the existing methods such as: Ayman et al.[12], Del-Fresno et al.[14] and Wu et al.[15] (which contain different homogeneity criterion) by applying them on simulated volumetric MRI datasets. We measure the WM of MRI slice#62 after performing the proposed algorithm and the existing ones as shown in Figure 5. Figure 5 shows the measure of WM of the proposed, Ayman et al.[12], Del-Fresno et al.[14] and Wu et al.[15] techniques when they are applied to original slice#62 with noise levels 1%, 3%, 5% and RF level 20%. Table 2 presents the accuracy of the proposed method compared to Ayman et al. [12], Del-Fresno et al.[14] and Wu et al.[15] techniques. In particular, although the segmentation quality logically deteriorates in the presence of noise and variations in intensity, the robustness of the present technique is highly satisfactory, compared with the results of other segmentation techniques.

## 5. Conclusion

In this paper, we have proposed an automatic threshold for region growing to segment MRIs containing weak boundaries. The proposed method has several advantages compared to previous segmentation strategies. One of the most important improvements is that the method gives an automatic threshold for different volumes data by using the pixels probability from the image. The growing process

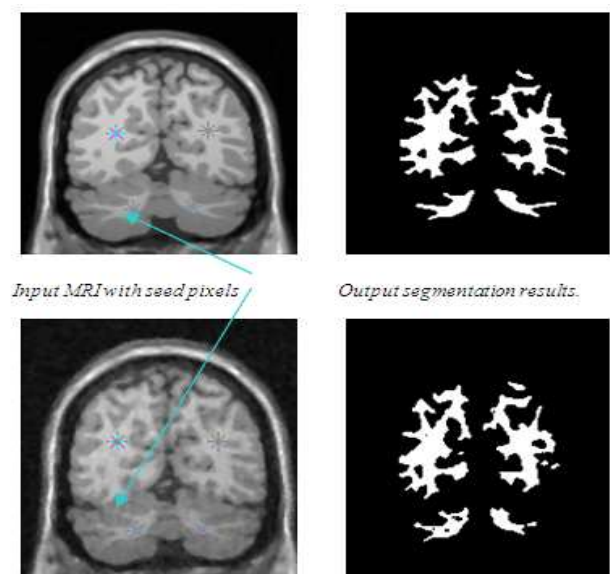


**Figure 3:** The input MRI (left) and output segmentation results (right), segmentation accuracy 93% and 91% respectively.

**Table 1:** The AOM for segmentations of WM on simulated T1-weighted MRI data with different situations of noise level and intensity non-uniformity(RF).

| Noise/RF | 0    | 20%  |
|----------|------|------|
| 0%       | 0.97 | 0.96 |
| 3%       | 0.95 | 0.96 |
| 5%       | 0.95 | 0.93 |
| 7%       | 0.93 | 0.92 |
| 9%       | 0.92 | 0.90 |

**Table 2:** AOM for WM using the proposed method, Ayman et al.[12], Del-Fresno et al.[14] and Wu et al.[15] techniques.

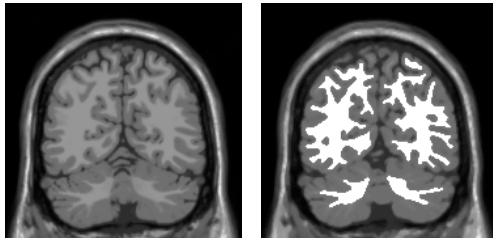
| RF                    | 20%  |      |      |
|-----------------------|------|------|------|
| Noise                 | 1%   | 3%   | 5%   |
| Ayman et al.[12]      | 0.95 | 0.94 | 0.87 |
| Del-Fresno et al.[14] | 0.94 | 0.89 | 0.87 |
| Wu et al.[15]         | 0.90 | 0.90 | 0.88 |
| The proposed method   | 0.98 | 0.95 | 0.94 |

incorporates information of the local neighborhood and probability of each voxel of the region. The proposed technique has been tested on the segmentation of complex MRI real images in order to extract the challenge application white matter (WM) tissues. We have used slice#62 and

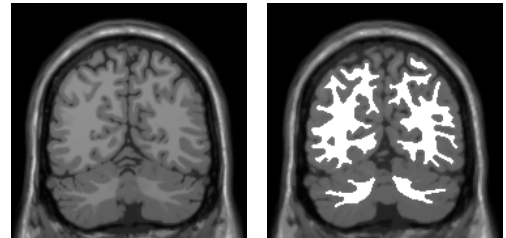
slice#63 with noise level 3%. These test images showed that segmentation results are much close to ground truth, the segmentation of white matter shows excellent performances exceeding 91%. To prove the efficiency of the proposed algorithm in segmenting the noisy images, the proposed algorithm has been applied to MRIs at noise levels (0%, 3%, 5%, 7%, and 9%) and RF levels (0% and 20%) which contain weak boundaries. These test images showed that segmentation results are much close to ground truth, the segmentation of white matter show excellent performances, the average exceeding 90%. We have noted that the proposed algorithm is succeeded to segment real images which have noise levels from 0% to 9% and RF levels from 0% to 20%.

Moreover, quantitative results are also given in our experiments. The superiority of the proposed algorithm is demonstrated by comparing its performance with more recent methods as: Ayman et al.[12], Del-Fresno et al.[14] and Wu et al.[15]. We noted that the segmentation accuracy of the proposed method increased by 3% at 1% noise and 7% at 5% noise for test images. It is clear that the accuracy of the proposed method is stable and is better than other approaches at big noise.

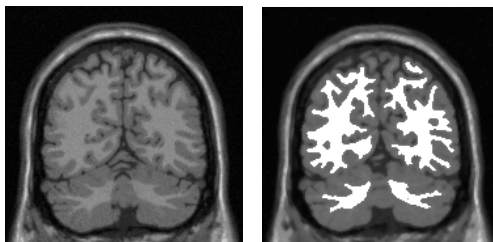
Further research is directed toward the improvement of the 3D version of the algorithm and its extension to the segmentation of 3D medical images with the consideration of the geometry structure of interesting objects and the statistical characteristics of sub-regions.



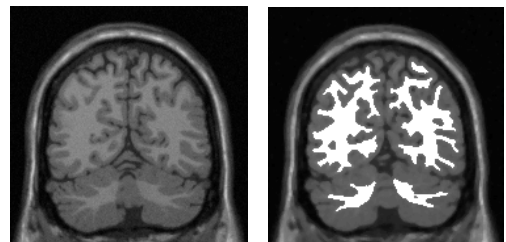
Noise =0% and RF=0%, AOM=0.97



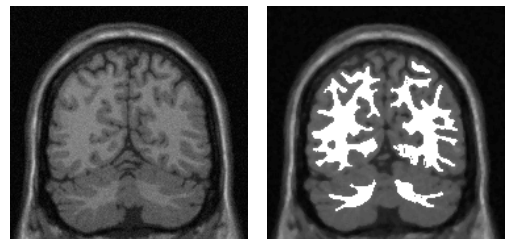
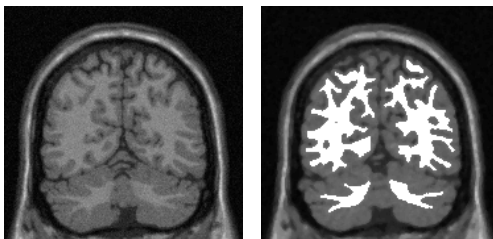
Noise =0% and RF=20%, AOM=0.96



Noise =3% and RF=0%, AOM=0.96



Noise =3% and RF=20%, AOM=0.95



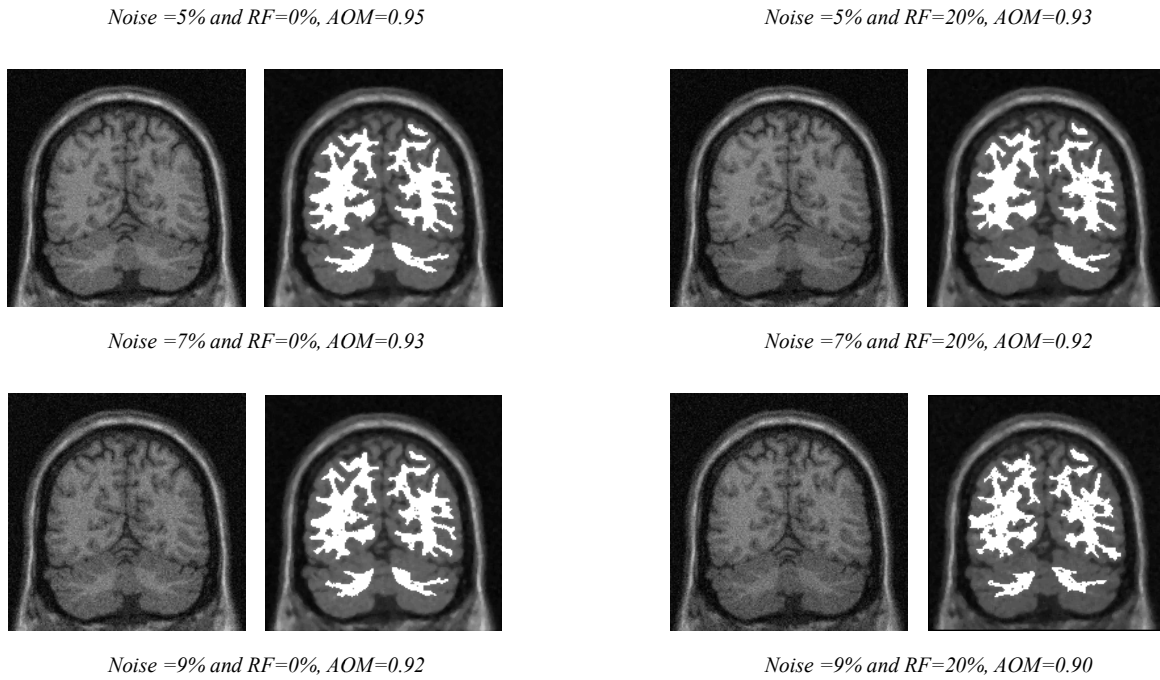


Figure 4: Original slice #62 and its segmentation results of WM for different noise and RF levels.

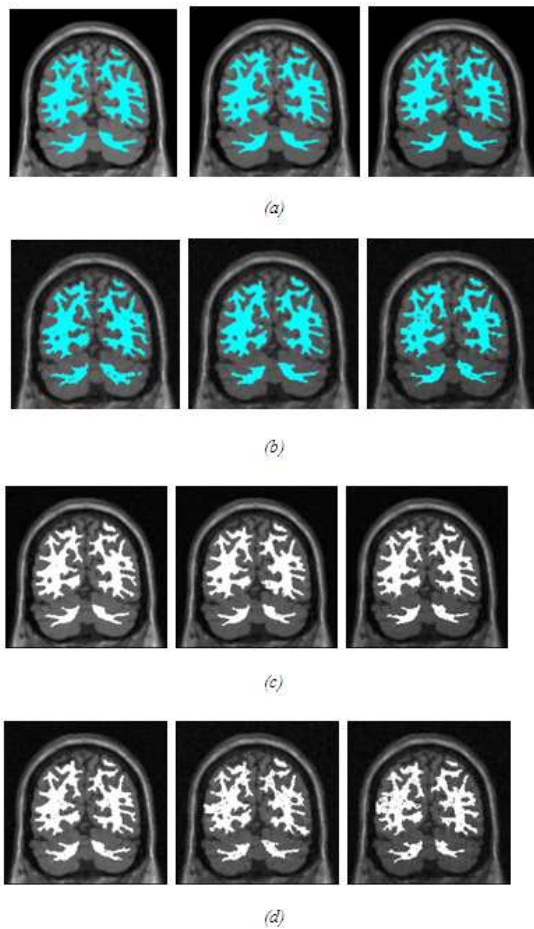


Figure 5: Segmentation of WM at noise levels 1%, 5% and 9% respectively with RF 20% : (a) The proposed method, (b) Ayman et al.[12], (c) Del-Fresno et al.[14], (d)Wu et al.[15].

## References

- [1] RB. Buxton, "Introduction to functional magnetic resonance imaging-principles and technique", Cambridge University Press, 2002.
- [2] Pham D. L., Xu C. and Prince J. L., "A survey of current methods in medical image segmentation", Annual Review of Biomedical Engineering, 1998.
- [3] O. Gloger, J. Kühn, A. Stanski, H. Völzke, and R. Puls, "A fully automatic three-step liver segmentation method on LDA-based probability maps for multiple contrast MR images", Magnetic Resonance Imaging, vol. 28, pp.882-897, 2010.
- [4] Z. Chen, "Histogram partition and interval thresholding for volumetric breast tissue segmentation", Computerized Medical Imaging and Graphics, vol. 32, pp. 1-10, 2008.
- [5] Li L., Gong J. and Chen W., "Gray-level image thresholding based on Fisher linear projection of two-dimensional histogram", Pattern Recognition, vol. 30, no. 5, pp. 743-749, 1997.
- [6] O. J. Tobias, and R. Seara, "Image segmentation by histogram thresholding using fuzzy sets", IEEE Trans. Image Process, vol. 11, no. 12, pp.1457-1465, 2002.
- [7] Rolf Adams, Leanne Bischof, "Seeded region growing", IEEE Trans. on PAMI, vol. 16, no. 6, pp.641 -647, 1994.
- [8] Andrew Mehnert, Paul Jackway, "An improved seeded region growing algorithm", Pattern Recognition Letters, vol. 18, pp.1065-1071, 1997.
- [9] A. Hojjatoleslami, and J. Kittler, "Region growing: a new approach", IEEE Transactions on Image Processing, vol.7, pp.1079-1084, 1998.
- [10] Y. L. Chang, and X. Li, "Adaptive image region growing",

- IEEE Transactions on Image Processing, vol.3, pp.868–873, 1994.
- [11] Jie Wu, Poehlman, S.; Noseworthy, M.D.; Kamath, M.V., "Texture feature based automated seeded region growing in abdominal MRI segmentation", International Conference on Biomedical Engineering and Informatics, Sanya, China, pp.27-30, 2008.
- [12] A. Ayman, , T. Funatomi, M. Minoh, Z. Elnomery, T. Okada, K. Togashi, T. Sakai and S. Yamada, "New region growing segmentation technique for MR images with weak boundaries", IEICE conference MI2010-79, JAPAN, pp.71-76, 2010.
- [13] Hong-Rui Wang, Jian-li Yang; Hai-jun Sun; Dong Chen; Xiu-Ling Liu, "An improved region growing method for medical image selection and evaluation based on Canny edge detection", Management and Service Science (MASS), pp.1-4, 2011.
- [14] M. Del-Fresno, M. Vénere, and A. Clause, "A combined region growing and deformable model method for extraction of closed surfaces in 3D CT and MRI scans", Computerized Medical Imaging and Graphics, vol.33, pp.369-376, 2009.
- [15] Wu Y. -T., Shih F. Y., Shi J., and Wu Yi.-T., "A top-down region dividing approach for image segmentation", Pattern Recognition, vol. 41, pp. 1948–1960, 2008.
- [16] Tang H., Wu E. X., Ma Q. Y., Gallagher D., Perera G. M. and Zhuang T., "MRI brain image segmentation by multi-resolution edge detection and region selection", Computerized Medical Imaging and Graphics, vol. 24, pp. 349–357, 2000.
- [17] E. A. Zanaty, Ahmed S. Ghiduk, "A novel approach based on genetic algorithms and region growing for magnetic resonance image (MRI) segmentation", ComSIS journal, In Press, 2013.
- [18] Muhammad Noorul Mubarak, M. Mohamed Sathik, S.Zulaikha Beevi, K. Revathy, "A hybrid region growing algorithm for medical image segmentation", International Journal of Computer Science & Information Technology (IJCSIT), vol. 4, no 3, 2012.
- [19] <http://www.bic.mni.mcgill.ca/brainweb/>
- [20] <http://pubimage.hcuge.ch:8080/>
- [21] P. Jaccard, "The distribution of flora in the alpine zone", New Phytol., vol.11, no.2, pp.37–50, 1912.
- [22] A. P. Zijdenbos, "MRI segmentation and the quantification of white matter lesions", PhD thesis, Vanderbilt University, Electrical Engineering Department, Nashville, Tennessee; December 1994.